Scientific Research Publishing

Journal of Geoscience and Environment Protection, 2024, 12, 28-45
https://www.scirp.org/journal/gep
ISSN Online: 2327-4344
ISSN Print: 2327-4336

Petrographic, Mineralogical and Geochemical Characterization of the Boundou-Waadé Bauxite Deposit (Sangaredi, Republic of Guinea)

Chontcheihon Virginie Traoré[1*], Mohamed Samuel Moriah Conté[1], Daouda Keita[2], Abdoulaye Kadiatou Diallo[1], Mamoudou Diallo[1], Mamoudou Conde[3]

[1]Laboratoire de Recherche Appliquee en Geosciences et Environnement, Departement des Services Geologiques, Institut Superieur des Mines et Geologie de Boke (ISMGB), Boke, Republique de Guinee
[2]Laboratoire de Recherche Appliquee en Geosciences et Environnement, Departement des Services Miniers, Institut Superieur des Mines et Geologie de Boke (ISMGB), Boke, Republique de Guinee
[3]Compagnie des Bauxites de Guinee (CBG), Departement Geologie, Sangaredi, Republique de Guinee
Email: *ingtraorevirginie92@gmail.com

How to cite this paper: Traoré, C. V., Conté, M. S. M., Keita, D., Diallo, A. K., Diallo, M., & Conde, M. (2024). Petrographic, Mineralogical and Geochemical Characterization of the Boundou-Waadé Bauxite Deposit (Sangaredi, Republic of Guinea). *Journal of Geoscience and Environment Protection, 12,* 28-45.
https://doi.org/10.4236/gep.2024.1212002

Received: August 6, 2024
Accepted: December 8, 2024
Published: December 11, 2024

Abstract

The demand for useful ores has been growing steadily, especially since there is increasing interest in bauxite ores. This growing demand is prompting researchers to justify a large number of research projects on bauxites. The aim of this work is to characterize the Boundou-Waadé bauxite deposit. The proposed methodology is mainly based on sample collection, stratigraphic logs, cross-sections and geological maps. Samples were analyzed at the Compagnie des Bauxites de Guinée laboratory. Geochemical data were processed using statistical methods. Devonian sedimentary formations and Mesozoic dolerites characterize the study area. The Boundou-Waadé bauxite deposit was developed on Devonian and Mesozoic formations. Stratigraphic logs show the succession of formations, with the bedrock overlain by the alteration crust. The bauxitic zone, the transition zone and the ferruginous laterites are the subject of petrographic studies, with both zones (bauxitic and transition) containing some ferriplantite. Mineralogical analysis clearly shows that gibbsite, goethite, alumogoethite, rutile and clay minerals are present. The geochemical study of the major elements shows that as SiO_2 and Fe_2O_3 content decreases, Al_2O_3 content increases and TiO_2 and Al_2O_3 content increases in the same direction.

Keywords

Bauxites Aleuro-Argillite, Dolerite, Gibbsite

1. Introduction

Bauxite, iron and gold mineralization is known and exploited in West Africa, particularly in Guinea (**Figure 1(a)**). West Africa and Brazil hold the world's largest reserves of lateritic bauxites (Boulange et al., 1990). Bauxite ore deposits are located on either side of the uplift axis of the West African shield (Bruno Boulanger and Millot, 1988). Guinea's abundance of resources has earned it the title of "geological scandal". In recent years, the demand for useful minerals has continued to grow, especially as there is growing interest in bauxite ores, which play an essential role in many fields such as industry and technology. However, the exploitation of bauxites is an economical option for the countries that own them, it justifies a high level of bauxite research. Bauxite ore is economically viable if it contains at least 40% Al_2O_3, less than 8% SiO_2, and the Al_2O_3/Fe_2O_3 ratio must be greater than (Njoya et al., 2017). Today, estimated bauxite reserves are around 40 billion tonnes, or 45% of the world's resources, located in the western part of the country (low coast) in an intracontinental basin known as the Paleozoic Bowé Basin (Mamedov et al., 2010). In terms of quality, the Sangarédi plateau is unique in the world for its Al_2O_3 (58% - 64%), SiO_2 0.8% - 1.5%, Fe_2O_3 < 4%; Mort terrain < 25 cm, more than 250 million tonnes over a surface area of 5 km^2 with an average bauxite thickness of 45 m. Boké bauxite province belongs to the Bowé Basin and comprises several bauxite plateaus, including the Boundou-Waadé plateau, surveyed at a scale of 1/200,000 (Samozvantsev et al., 1976). However, previous work has revealed the presence of three (3) types of bauxite on the Boundou-Waade deposit: the residual laterite type, the sedimentary type and the chemogenic type. Today, the bauxite mined by CBG is of the residual type, representing 75% of bauxite reserves. Very few scientific studies are available on these bauxite deposits, which makes their development complex. The aim of the present work is to study the petrography, geochemistry and mineralogy of bauxite samples with a view to their potential benefit.

2. Geological Setting

2.1. Geology of the Study Area

The prefecture of Boké is located in northwestern Guinea (**Figure 1(b)**) between latitudes 10˚30' and 11˚45' north, and longitudes 13˚45' and 15˚00 west. It covers 11,453 km^2 (Mamedov et al., 2010) and belongs to the Lower Guinea natural zone. The Boké region is made up of sedimentary formations of the Plateformian cover, crossed by numerous Mesozoic intrusions. This sedimentary cover is identified by the Ordovician formations, which are marked by fine quartz sandstones, sometimes with aleurolite intercalation, observed to the southwest (Seliverstov, 1970). The Silurian formations are represented by finely bedded black argillites, compact argillites, aleurolites and lenses of micro oolitic iron with intercalation of quartz sandstones (Seliverstov, 1970). The Devonian is underlain by Silurian argillites and aleurolites represented by quartz sandstones (Samozvantsev et al., 1976). At the end of the Paleozoic and Mesozoic, the study region experienced intense

tectonic activity linked to the break-up of the Gondwanan continent and the opening of the Atlantic. This activation is marked by the formation of a system of NE-SW transform faults and several secondary faults, through which intrusions have accessed. These magmatic intrusions are represented by dolerites (Boufeev et al., 1970; Samozvantsev et al., 1976). There are Cenozoic marine formations (quartz sands, bedded clays) and Paleogene weathering crusts resting on Paleozoic formations. The Neogene is characterized by conglomerates that lie concordantly on the Paleogene. Quaternary deposits are represented by sands, sandy silts, marine kaolinitic clays, fluvio-lacustrine clays and sands. These deposits are found on the coastal plain and sometimes in the river valleys (Figure 1(c)).

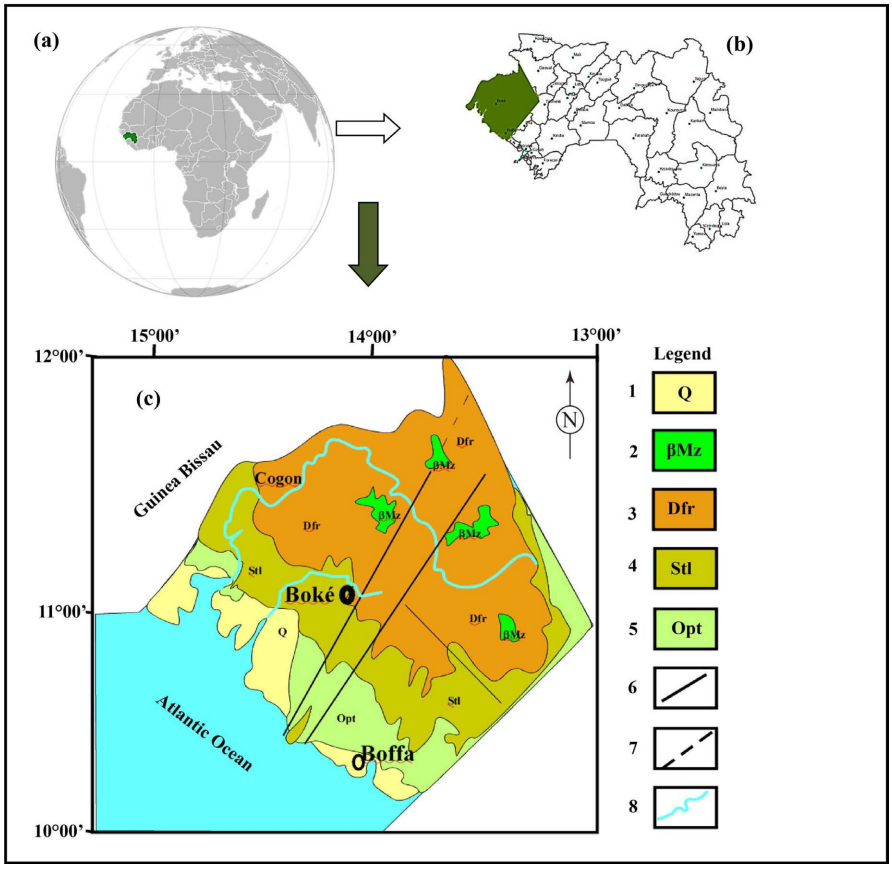

Figure 1. Presentation of the study region; (a) Location of Guinea; (b) Location of the study region; (c) Geological map of the study region. Cenozoic: 1—Undifferentiated deposit, alluvial clayey sands and sandy silts with gravels, pebbles and gravels, clayey sands and sandy silts with clayey arena and pebbles, deluvial-proluvial. Marine silt, clays, clayey sands and sands. Mesozoic: 2—Dolerite; gabbro-dolerites; cogon-diabase; rarely granophyres. Paleozoic: 3—Dfr: Faro suite, aleurolite, mudstone, sandstone. 4—Stl: Pêlemêle suite, argillite, aleurolite. 5—Opt: Pita suite, sandstone, quartzite and oligomictes, often oblique. Aleurolite lenses, gravites, conglomerates. 6—Subvertical faults. 7—Fault supposedly under the mantle of younger rocks. 8—Watercourses.

2.2. Geology of the Boundou-Waadé Deposit

The Boundou-Waadé bauxite deposit is represented by Devonian aleuro-

argillites, argillites and aleurolites into which Mesozoic dolerite sills and dykes are injected (Samozvantsev et al., 1976). On the deposit under study (**Figure 2**), the oldest faults strike northwest and north-south, while northeast-trending brittle dislocations are associated with recent transform faults. Northwest- and northeast-trending faults are the best developed. Tectonic activation occurred during the neotectonic phase when inherited landforms were established (Samozvantsev et al., 1976). The Mesozoic tectonomagmatic reactivation of the source rocks the Boundou-Waadé favored the emplacement of dolerite sills. These sills, of modest dimensions (4 - 10 m), are sub-concordant and gently sloping in relation to the surrounding Devonian sedimentary rocks (Mamedov et al., 2010). They alternate with intercalation of the sedimentary rocks of the Faro suite, whose thickness is comparable to that of the lateritic cover. The deposit under study is associated with the core of the Bowé syncline (**Figure 2**).

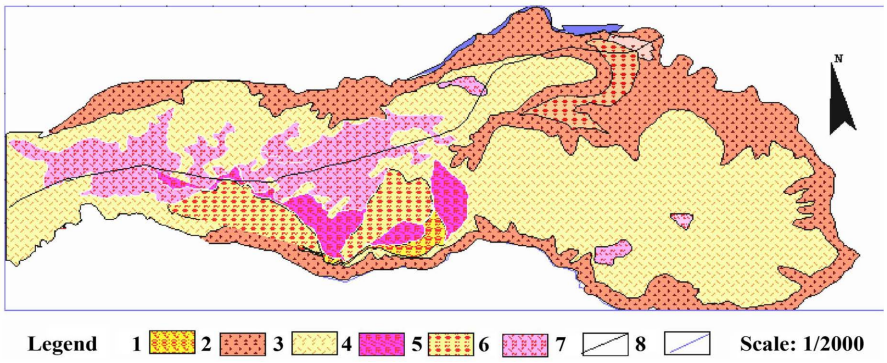

Figure 2. Geological map of the deposit modified from (Mamedov et al., 2010). 1—Gravelo-conglomeratic bauxites derived from Sangarédi series deposits; 2—Middle Miocene post-sedimentary laterite formation overlying dolerites; 3—Ferruginous laterites of the transition zone derived from aleuro-argilites; 4—Massive gelomorphic bauxites derived from dolerites; 5—Gravelly gravelly bauxites derived from Sangarédi series deposits; 6—Pseudomorphic bauxites derived from dolerites; 7—Faults; 8—Watercourses.

3. Materials and Methods

3.1. Materiel

The main material studied is the Boundou-Waadé bauxite deposit. To carry out this study, the following tools were used:

- Estwing hammer and an Atlas Copco drill to take samples;
- Canvas software to digitize maps and stratigraphic logs.
- ADP-1 diffractometer to determine mineralogical composition;
- Polarized microscope for petrographic analysis of samples;
- ICP-AES spectrometer to identify major elements;
- Triplot v4.1.2 software for triangular diagrams and Statigraphic Centurion_18.1.12 software for geochemical data processing.

3.2. Methods

During our internship from January 24 to March 30, 2020 at Compagnie of

Bauxites in Guinea, geological observations and studies (core analysis, stratigraphy, etc.) were carried out.

- Samples were then taken from the Boundou-Waadé deposit. The samples were sent to the mechanical laboratory for preliminary processing and then to the CBG laboratory in Kamsar for analytical study. A total of around seventy (70) samples were collected for macroscopic and microscopic analysis. Polarizing microscopy of lateritic rocks presents difficulties due to the (sub-microscopic) size of the phases and the presence of opaque sectors in highly ferruginous varieties. For this reason, the most interesting samples were analyzed by electron microscope and also by microprobe. These analyses were carried out at the Chair of Petrology and Mineralogy at Moscow's Lomonosov Federal University.
- Twelve (12) samples were analyzed by X-ray diffraction to determine the mineralogical composition. Subsequently, 12 samples were brought into play to identify the major elements in bauxites. The method consists of etching the sample on a hot plate in three stages: first with the mixture (HF and HCL), then with the mixed (HN03 + HCL) in by HCL.
- Bauxite samples were analyzed at the Institute of Steel and Alloys, Moscow, Russia, using inductively coupled plasma atomic emission spectrometry (ICP-AES). (ICP-AES) for the detection of major elements. All samples were plotted in triangular diagrams according to (Al_2O_3-SiO_2-Fe_2O_3), which made it possible to classify the samples according to these three categories. In short, statistical methods made it possible to analyze geochemical data.

4. Results

4.1. Stratigraphic Results

The Boundou-Waadé deposit is underlain by ferruginous bauxites 1.5 to 3 m thick at the surface, covered in places by vegetation. Analysis of stratigraphic logs C, D, E, H and J (**Figure 3**) shows two (2) types of formation: source rocks at the base, more than 1 m thick, topped by the alteration crust (Bhukte et al., 2020). This weathering crust is subdivided into four (4) distinct horizons (Sidibe and Yalcin, 2019): from bottom to top, there is the initial decomposition horizon (4 m thick), the clay horizon (1.5 m to 3 m), the transition zone (3 m to 7.5 m), and the free oxide or bauxite zone (9.5 m) (**Figure 3**). This bauxite zone is marked by gelified and lateritic bauxites. Isolated intercalation of nodular ferriplantites is observed.

4.2. Petrographic Results

- **Bauxites**

Macroscopic and microscopic studies were carried out on bauxites and ferruginous laterites.

The Boundou-Waadé deposit contains two (2) groups of bauxites:

- Lateritic bauxites (*in-situ*) subdivided into two (2) litho-genetic types according to their texturo-structural features:

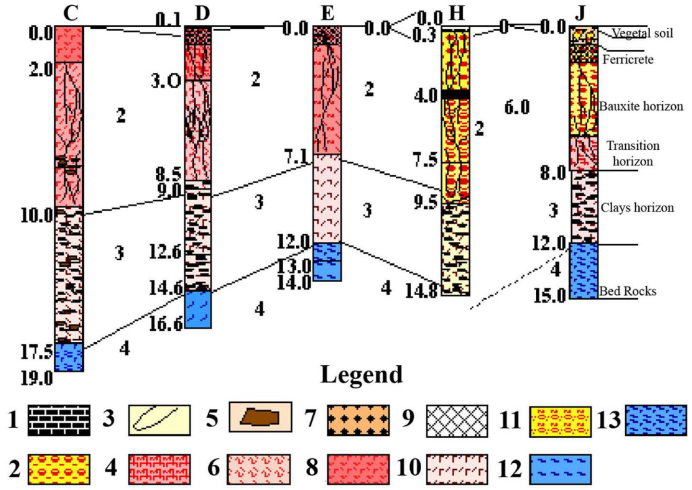

Figure 3. Stratigraphic logs of boreholes C, D, E, H and J (Mamedov et al., 2010) (modified after). C—deriving from dolerites; with weakly gelled bauxites and classic apodoleritic bauxites; D—deriving from the recurrence of dolerites and aleuro-argillites with gelomorphic and gelled apodoleritic bauxites; E—deriving from the recurrence of aleuro-argillites from the upper member of the Faro suite and dolerites; with structural gelled bauxites; H—derived from deposits of the Sangarédi series, underlain by dolerites; with gravelly and gravelly-conglomeratic bauxites derived from the Sangarédi series; J—derived from deposits of the Sangarédi series, underlain by dolerites; with gravelly bauxites derived from the Sangarédi series and apodoleritic gelomorphic bauxites. 1—Vegetated soil; 2—Strands of ferruginous laterites, in places with nests of clay laterites; 3—Red and tobacco yellow ferriplantites; 4—Ferruginous laterites (curasse); 5—Ferritization zone; 6—Gravelly gravelly bauxites derived from deposits of the Sangarédi series; 7—Gravelly conglomeratic bauxites derived from deposits of the Sangarédi series; 8—Massive gelomorphic bauxites derived from dolerites; 9—Pseudomorphic gelled bauxites derived from aleuro-argilites; 10—Pseudomorphic gelled bauxites derived from dolerites; 11—Pseudomorphic bauxites derived from dolerites; 12—Ferruginous dolerite-derived transition zone bauxites; 13—Pseudomorphic white, grayish-white and pink kaolinitic clays derived from aleuro-argilites.

- bauxites formed at the expense of aleurolites, Devonian clays (**Figure 4(a)** and **Figure 4(c)**).

  These bauxites are most often referred to as structural bauxites;
- bauxites formed from Mesozoic dolerites (**Figure 4(b)** and **Figure 4(d)**).

Both types of bauxite are characterized by their low quality and low aluminum monohydrate content. This is due to the predominance of gibbsite. Alumogoethite has a low alumina content. Titanomagnetite is present in apodoleritic bauxites. Rutile and anatase are typical for bauxites developed at the expense of Devonian rocks (**Figure 5(a)** and **Figure 5(b)**). Lateritic bauxites can be distinguished by their textural features and platelet-like divisions for structural bauxites (**Figure 5(d)**) and shell-like divisions for apodoleritic bauxites.

Chemogenic bauxites represent only 2%, and are simply the product of the chemical redistribution of elements at the base of lateritic bauxites. The latter is subdivided into two (2): gelomorphic bauxites, which are less widespread on the deposit, and gelified bauxites, which are more widespread (**Figure 5(c)**). They have a massive texture and a microcrystalline structure. In comparison with

lateritic bauxites, they are similar in textural features, with a slight difference in pink-white coloration; lighter pink.

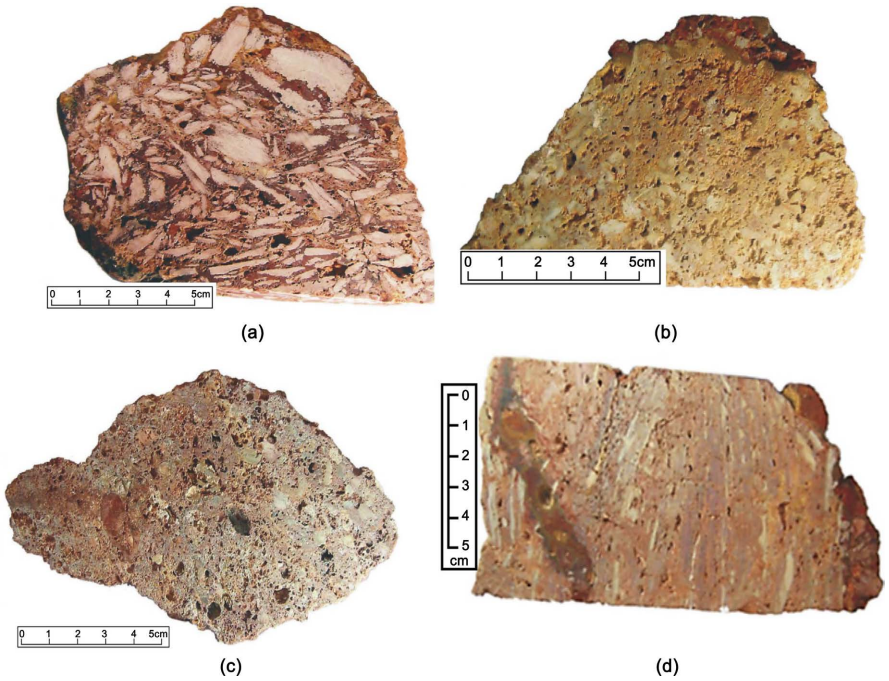

Figure 4. (a)—Lateritic bauxites derived aleuro-argillites; (b)—Apodoleritic gelled bauxites; (c)—Gelomorphic bauxites from the Sangarédi series; (d)—Apodoleritic gelled bauxites.

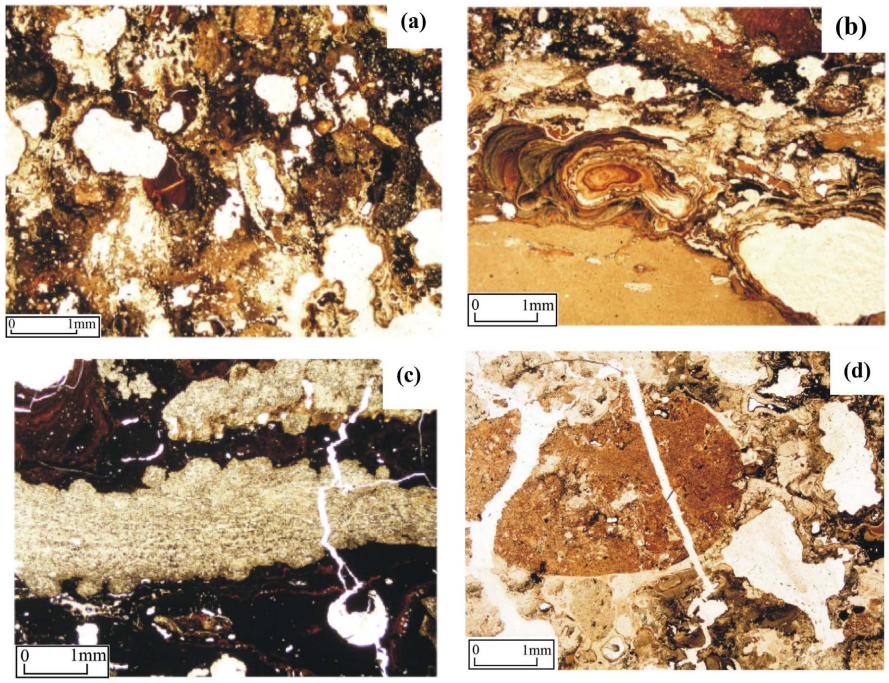

Figure 5. (a)—Lateritic bauxites derived aleuro-argillites; (b)—Lateritic bauxites derived from the Sangarédi series; (c)—Gelified bauxites derived aleuro-argillites; (d)—Apodoleritic gelled bauxites.

- **Ferruginous laterites from the upper part of the bauxite interval**

Ferruginous laterites have a massive, cavernous texture and an aphanitic colomorphic structure (bauxite derived from dolerites). As a rule, they are composed of ferrigels and hematogels that form rhythmically zoned patches encrusting the walls of cracks and caverns. Large grains of newly-formed secondary gibbsite, 2 - 3 mm in diameter, are also found.

- **Ferruginous laterites of the transition zone developed at the expense of aleuro-argilites of the upper limb of the Faro suite**

They have a pseudobrecciated texture with yellow, yellowish-red coloration and pores. Fragments range in size from 1 - 2 to 6 - 9 mm, with a sharp-edged shape and a very bright dark-red color. The cement is composed of hematogel and ferrigel with a yellowish-red, variable-yellow color. The fragments have a massive texture and an aphanitic collomorphic structure, occupying a large part (80% - 90% and more) composed of ferruginous minerals (goethite, hematite). The cement is developed in the form of veinlets, and presents an aphanitic texture and a collomorphic structure. It is semi-transparent under piercing light. The cement is composed of ferrialumogel (Figure 6).

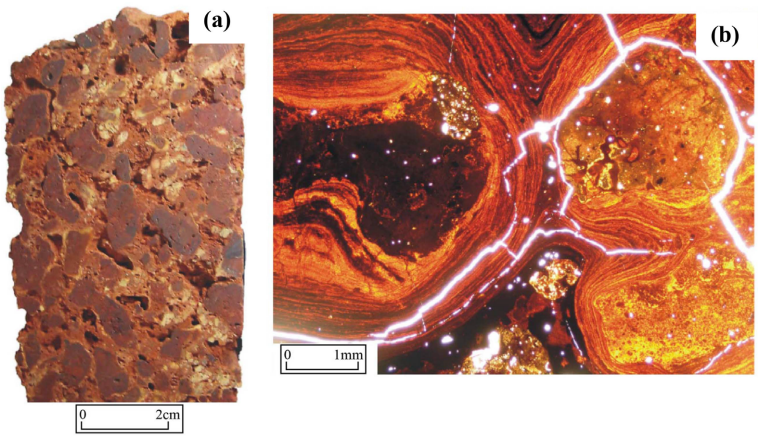

Figure 6. Ferruginous laterites from the upper part of the interval.

4.3. Mineralogical Results

XRD analysis shows that mineralogical composition is similar in all log bauxites (C, D, E, H, J). The results of quantitative phase analysis are given in tables (1 and 2); these values represent the relative quantities of crystalline and amorphous phases normalized to 100%. Boehmite and diaspore are absent in some samples. The bauxitic horizon of log C, D and E—most samples contain gibbsite, alumogoethite, goethite, hematite, anatase and rutile, accompanied by a mineralization of hydromica.

Several mineral combinations: kaolinite (C06 and C07); kaolinite, quartz (C07); kaolinite, quartz and hydromica (E01) (Table 1). In the clay horizon of sections C, D and E, most samples contain kaolinite, quartz and hydromica. In the Log H and J bauxitic horizons, most of the samples contain kaolinite, quartz and

hydromica. contain gibbsite, alumogoethite, goethite and hematite, accompanied by one or more minerals such as rutile and kaolinite (J01) (Table 2). In the clay horizon. From the results of mineralogical analysis (Table 1 and Table 2), given the absence of boehmite and diaspore, we can deduce that gibbsite is the economic mineral for aluminum at Boundou-Waadé.

4.4. Geochemical Results

Geochemical analysis clearly shows that Boundou-Waadée bauxite is essentially composed of: Al_2O_3 (23% - 68.4%); Fe_2O_3 (3.00% - 51.25%); SiO_2 (0.5% - 2.9%) and TiO_2 (1.32% - 8.1%).

Alkaline and alkaline-earth: FeO (0.04% - 0.43%), CaO (0.05% - 0.16%), MgO (0.05% - 0.42%). MnO (0.0064% - 0.072%). K_2O (0.002% - 0.5%). Na_2O (0.01% - 0.7%). P_2O_5 (0% - 0.1%) et PAF (011% - 29.5%) have low values (Table 3).

Table 1. Table type styles Logs C, D, E mineralogical result.

		Bauxitic horizon											Clay horizon				
Mineral	Chemical formulas	C02	C03	C04	C05	C06	D03	D04	D05	E02	E03	E04	C01	D01	D02	C07	E01
Gibbsite	$Al(OH)_3$	31	12	29	25	22	80	69	10	77	40	61	48	82	25	-	10
Boehmite	AlO(OH)	-	-	2	-	-	1	-	-	2	3	-	35	2	3	-	2
Diaspore	AlO(OH)	-	-	-	-	-	-	-	-	-	-	-	-	-	-	-	-
Alumogoethite Goéthite	FeO(OH)	6	22	12	6	8	4	11	19	5	10	4	8	4	21	16	16
Hématite	Fe_2O_3	7	-	5	15	13	11	15	-	6	12	4	8	3	5	-	6
Anatase	TiO_2	1	-	1	0.5	1	15	-	-	3	0.5	1	0.5	3	1	-	-
Rutile	TiO_2	1	-	1	0.5	1	15	-	-	3	0.5	1	0.5	3	1	-	-
Kaolinite	$Al_2Si_2O_3(OH)_4$	-	-	-	-	7	-	1	-	-	-	-	-	-	-	50	-
Quartz	SiO_2	-	-	2	-	2	-	-	-	-	-	-	-	-	-	2	-
Hydromica	(K, H_3O) (Al, Mg, Fe)$_2$ (Si, Al)$_4O_{10}$[(OH)$_2$(H_2O)]	-	-	-	-	-	-	-	-	-	-	-	-	-	-	-	2
Chlorite	(Fe, Mg, Al)$_6$ (Si, Al)$_4O_{10}(OH)_8$	-	-	-	-	-	-	-	-	-	-	-	-	-	-	-	-
Phase R/a		54	66	48	54	46	-	-	70	5	5	33	33	3	44	32	64

Table 2. Log H, J mineralogical result.

		Bauxitic horizon									*Clay horizon*			
Mineral	Chemical formulas	H01	H02	H03	H04	H05	H06	H07	H08	H09	J01	J02	J03	J04
Gibbsite	$Al(OH)_3$	75	57	42	42	42	36	77	16	16	35	32	-	-
Boehmite	AlO(OH)	17	18	6	6	6	7	16	-	-	-	-	-	-
Diaspore	AlO(OH)	3.52	2	2.61	3.4	3.1	19.9	7.3	43	73.5	11	-	-	-
Alumogoethite Goéthite	FeO(OH)	-	-	-	-	-	-	-	-	-	-	-	-	-

Continued

Hématite	Fe_2O_3	-	-	-	-	-	-	-	-	-	-	-	-	-	-
Anatase	TiO_2	-	-	-	-	1	-	-	-	-	-	-	-	-	-
Rutile	TiO_2	-	-	-	-	1	-	-	-	-	-	-	-	-	-
Kaolinite	$Al_2Si_2O_3(OH)_4$	-	-	-	-	-	-	-	-	-	-	-	-	-	-
Quartz	SiO_2	-	-	-	-	-	-	-	-	-	-	-	-	-	-
Hydromica	$(K, H_3O)(Al, Mg, Fe)_2(Si, Al)_4O_{10}[(OH)_2(H_2O)]$	-	-	-	-	-	-	-	-	-	-	-	-	-	-
Chlorite	$(Fe, Mg, Al)_6(Si, Al)_4O_{10}(OH)_8$	-	-	-	-	-	-	-	-	-	-	-	-	-	-
Phase R/a		-	-	-	-	-	0.73	0.19	0.21	0.7	63	-	-	-	

Clays (C07, J04 and J03) have component values ranging from 0.05% to 41.25%. Al_2O_3 (24.07% - 29.9%). SiO_2 (32.5% - 41.25%) Fe_2O_3 (18.6% - 21%) TiO_2 (1.68% - 2.52%) FeO (0.13% - 0.16%) CaO (0.09% - 0.15%) MgO (0.05% - 0.42%) MnO (0.08% - 0.23%) K_2O (0%) Na_2O (0%) P_2O_5 et (0%) and (13.22% - 15.5%) PAF. While the aleuro-argillite samples: (CO5; CO6; H08; JO1; JO2) have respective values in: Al_2O_3 28.58% and 41.47%; SiO_2 1.72% and 7.00%; Fe_2O_3 30.8% and 48.50%; TiO_2 1.50% and 2.68%; FeO 0.04% and 0.43%; CaO 0.05% and 0.08%; MgO 0.05% and 0.05%; MnO 0.02% and 0.04%; K_2O 0.00% and 0.03%; Na_2O 0.00% and 0.03%; $P_2O_5 \leq 0.05\%$ with a PAF ranging from 0.21% to 23.88% (Table 3).

Table 3. Chemical analysis results.

(a)

	Gelified bauxites											Lateritic bauxites				Ferriplantitis				
N0Ech.	C04	D03	D04	E02	H01	H03	H04	H05	H06	H07	C02	D01	D02	E01	H02	J01	J02	C03	D05	H09
Al_2O_3 (%)	53.6	54.69	45.6	59.77	60.6	58	68.4	61.5	52	61.4	38.94	53.2	25.83	23	40.1	37.48	41.47	15.58	16.3	10.78
SiO_2	0.72	0.57	0.57	1.95	2.9	0.9	0.4	0.5	0.79	1.4	1.5	0.92	1.6	4.05	0.82	22	2.15	2.85	2.75	2.6
Fe_2O_3	1.84	9.5	25	6.95	3.8	11	3	3.35	19.9	7.3	31	8.2	50.75	51.25	35.8	37.5	30.8	62.7	60	73.5
TiO_2	2.1	4.95	3.37	2.9	3.52	2.6	3.4	3.1	2.65	3.22	4.02	8.1	1.8	1.4	2	1.5	1.52	0.7	1.25	0.58
FeO	0.043	0.23	0.27	0.057	0.04	0	0.06	0.1	0.11	0.1	0.14	0.07	0.026	0.19	0.09	0.43	0.42	0.06	0.09	0.69
CaO	0.05	0.065	0.05	0.055	0.05	0	0.12	0.05	0.08	0.11	0.1	0.05	0.15	0.065	0.05	0.065	0.08	0.05	0.07	0.05
MgO	0.05	0.05	0.05	0.05	0.05	0	0.05	0.05	0.05	0.05	0.05	0.06	0.05	0.06	0.05	0.05	0.05	0.05	0.05	0.05
MnO	0.022	0.021	0.072	0.015	0.02	0	0.02	0.01	0.02	0.01	0.062	0.02	0.023	0.019	0.02	0.027	0.022	0.02	0.016	0.02
K_2O	0	0.01	0.01	0.04	0.01	0	0	0	0.02	0.03	0	0.002	0.01	0.01	0.05	0.02	0	0	0.02	0.14
Na_2O	0	0.02	0.02	0.03	0.03	0.05	0	0	0	0.02	0.04	0	0.01	0.04	0.07	0.05	0	0	0.04	0.07
P_2O_5	0	0.06	0.01	0.09	0.05	0	0	0	0.05	0.05	0	0.08	0.5	0.29	0.05	0	0	0	0.039	0.05
PAF	29.9	29.37	25.8	26.4	0.11	0	0	0	0.73	0.19	24.43	28.9	19.67	13.43	0.5	21.61	23.88	17.55	17.9	0.9

(b)

	Ferruginous laterite			Clay		Aleuro-Argillites			
N0Ech.	C07	E04	H08	J03	J04	C01	C05	C06	E03
Al_2O_3 (%)	29.9	54.8	31.9	27.69	24.07	32.79	28.58	29.8	38.3

Continued

SiO_2	32.5	1.47	1.75	38.12	41.25	2.91.72	1.72	7	0.74
Fe_2O_3	21	10.5	43	18.6	18.9	41	48.5	42.8	37
TiO_2	2.52	1.9	1.9	1.78	1.68	1.32	2.68	2.68	1.82
FeO	0.16	0.04	0.04	0.13	0.14	0.072	0.14	0.19	0.29
CaO	0.09	0.16	0.05	0.12	0.15	0.05	0.05	0.05	0.05
MgO	0.05	0.05	0.05	0.32	0.42	0.05	0.05	0.05	0.05
MnO	0.08	0.02	0.04	0.23	0.22	0.0064	0.024	0.02	0.03
K_2O	0	0.01	0.03	0	0	0	0	0	0
Na_2O	0	0.02	0.03	0	0	0	0	0	0
P_2O_5	0	0.1	0.05	0	0	0	0	0	0
PAF	14.5	0.11	0.28	13.85	13.22	21.77	18.52	17.7	29.5

According to the mineralogical classification (Aleva, 1994), all bauxitic samples (C02, C04, D04, H01, H03, H04, H05, H07, D01 and E04) from the Boundou-Waadée plateau fall into the bauxite and ferric bauxite fields (**Figure 7**). The argillite samples (C07, J04 and J03) fall in the ferrite and laterite fields. Ferriplantites (C03, D05, H09) and ferruginous laterites (C07 and H08) fall into the ferrite field. We note that some clay samples (C07, J03, J04) fall into the kaolinite field, while some clays (D01, D03, E02 and E04) and aleuro-argillite (C07) fall into the bauxitic kaolinite field (**Figure 7**).

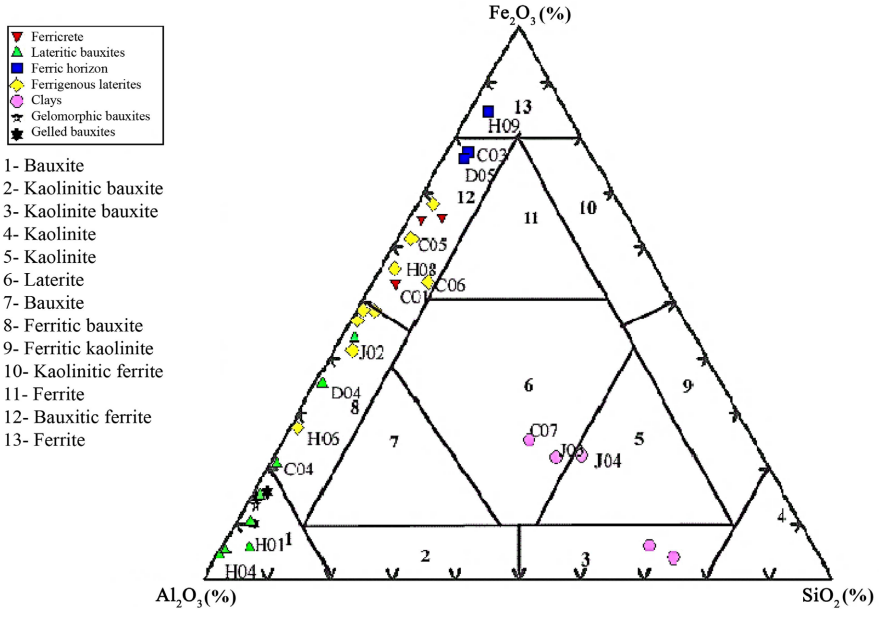

Figure 7. Triangular diagram between Al_2O_3-Fe_2O_3-SiO_2 (Aleva, 1994).

The triangular diagram of the degree of lateritization of bauxites by (Schellmann, 1986) shows that most samples (C05, C06, J01, J02, E03, H02, H06, H08, C01, D02, E01, C02, C04, D04, H01, H03 and H04) from Boundou-Waadé are strongly lateritized (**Figure 8**), while samples (C01, D02, E01, D01, D03, E03, E04) are weakly

lateritized. A bauxitic sample (E02) lies at the boundary between strong and moderate lateritization. Finally, a clay sample (J04) lies in the kaolinization band (**Figure 8**).

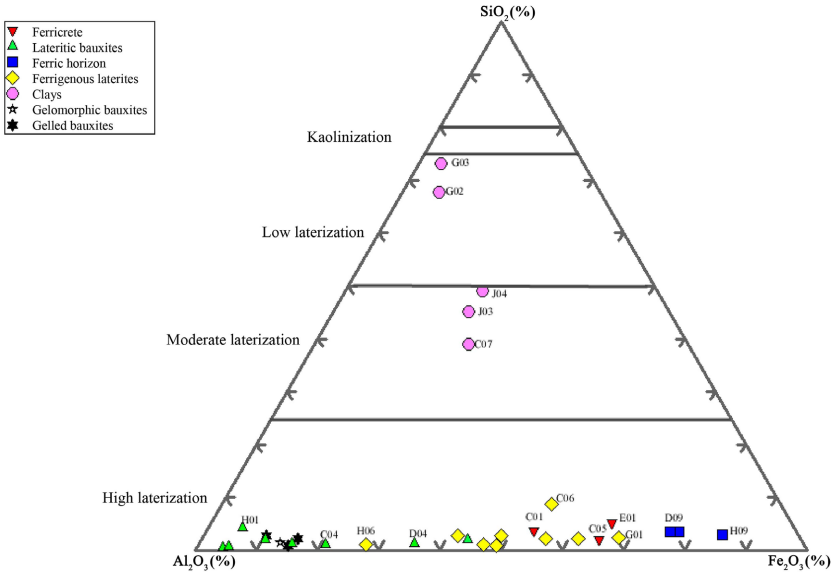

Figure 8. Triangular diagram between Al_2O_3-Fe_2O_3-SiO_2 (Schellmann, 1986).

In the classification diagram of (Boulange et al., 1996), all the bauxite samples (C02, C04, D04, H01, H03, H04, H05, H07, C05, C06, J02, E03) from Boundouwaadé fall within the bauxite and ferruginous bauxite fields. Only one bauxitic sample (E04) lies between the two bauxite fields (**Figure 9**). Ferruginous laterites (J02 and J04) lie between ferruginous and kaolinitic bauxites. The ferriplantites (C03, D05, H09) lie between the kaolinitic interval. In short, the clays (C07, J03, J04) and aleuro-argilites (CO7) are in the kaolinitic field (**Figure 9**).

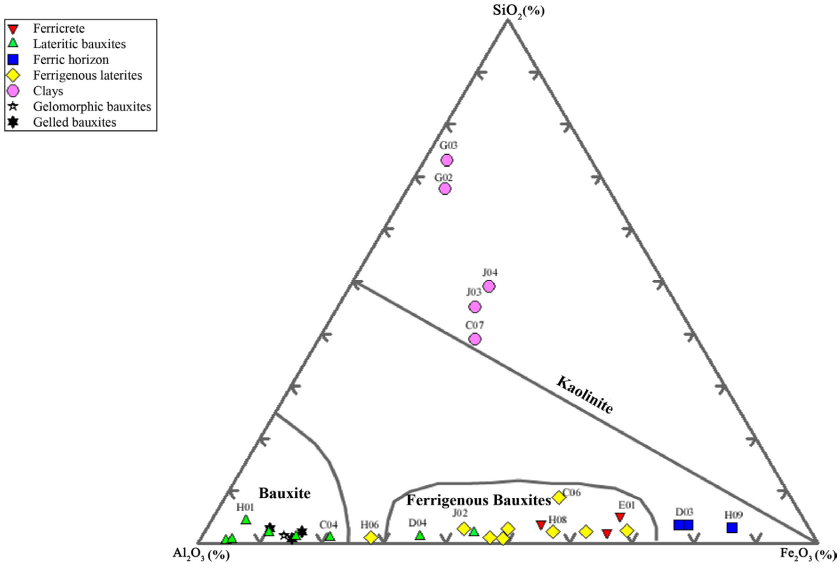

Figure 9. Triangular diagram between Al_2O_3-Fe_2O_3-SiO_2 (Boulange et al., 1996).

In the classification diagram of (Tardy, 1997), the geochemical dismantling trajectories demonstrate numerous trends followed during the bauxitization process: kaolinite preservation, deferruginization, kaolinite destruction and dehydration (**Figure 10**). Thus, the clay and aleuro-argillite samples (C07; J03; J04) follow the kaolinite preservation trend; in addition, the ferruginous laterite samples (C05; C06; H08; J01; J02) lie in the ferruginous shadow zone. Finally, the bauxite samples (C01; D02; E01; C02; C04; D01; D03; D04; E02; E03; E04; H01; H02; H03; H04; H05; H06; H07) follow the trend of kaolinite destruction, which explains why bauxites from the Boundou-Waadée deposit originate from the destruction of kaolinite (**Figure 10**).

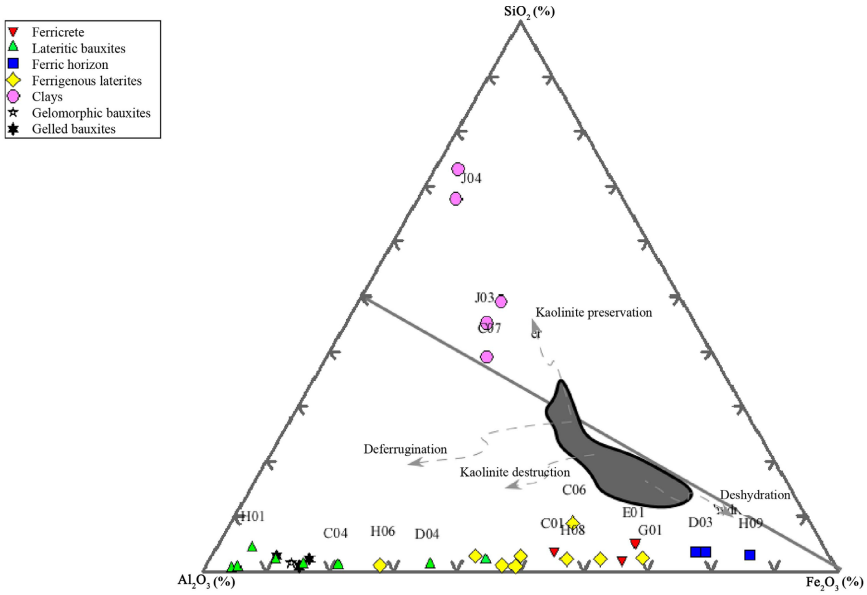

Figure 10. Triangular diagram between Al_2O_3-Fe_2O_3-SiO_2 from (Tardy, 1997).

The correlation diagrams for SiO_2, Fe_2O_3 and TiO_2 were plotted against Al_2O_3, the main chemical element, to study the behavior of the elements. The correlation diagrams for SiO_2, Fe_2O_3 and TiO_2 as a function of logs C, D, E, H and J are virtually identical (**Figure 11**). In logs C, D and E, SiO_2 content remains low despite high Al_2O_3 content, while Fe_2O_3 and Al_2O_3 content increases in these logs. Sample C07 has a high quartz content. Overall, they show low values in logs C, D and E. This can be explained by the fact that the content is constant in these logs, indicating a negative correlation on the other hand, in these same logs, Fe_2O_3 content shows a positive correlation with Al_2O_3. Whereas TiO_2 content shows a negative correlation with Al_2O_3 in these logs. In log H, the SiO_2 and TiO_2 versus Al_2O_3 plots show that their content decreases with Al_2O_3, indicating a negative correlation; while the Fe_2O_3 vs. Al_2O_3 diagrams show that Fe_2O_3 content increases with Al_2O_3, indicating a positive correlation. On the other hand, in log J, SiO_2 and Fe_2O_3 diagrams as a function of Al_2O_3 show that contents decrease with Al_2O_3 while TiO_2 increases with Al_2O_3, indicating a positive correlation. This positive correlation

can be explained by the fact that rutile, anatase and gibbsite contents are increasing (Figure 11). Thus, in bauxitic horizons, the major element correlation diagrams show silica leaching and residual enrichment in aluminum and titanium.

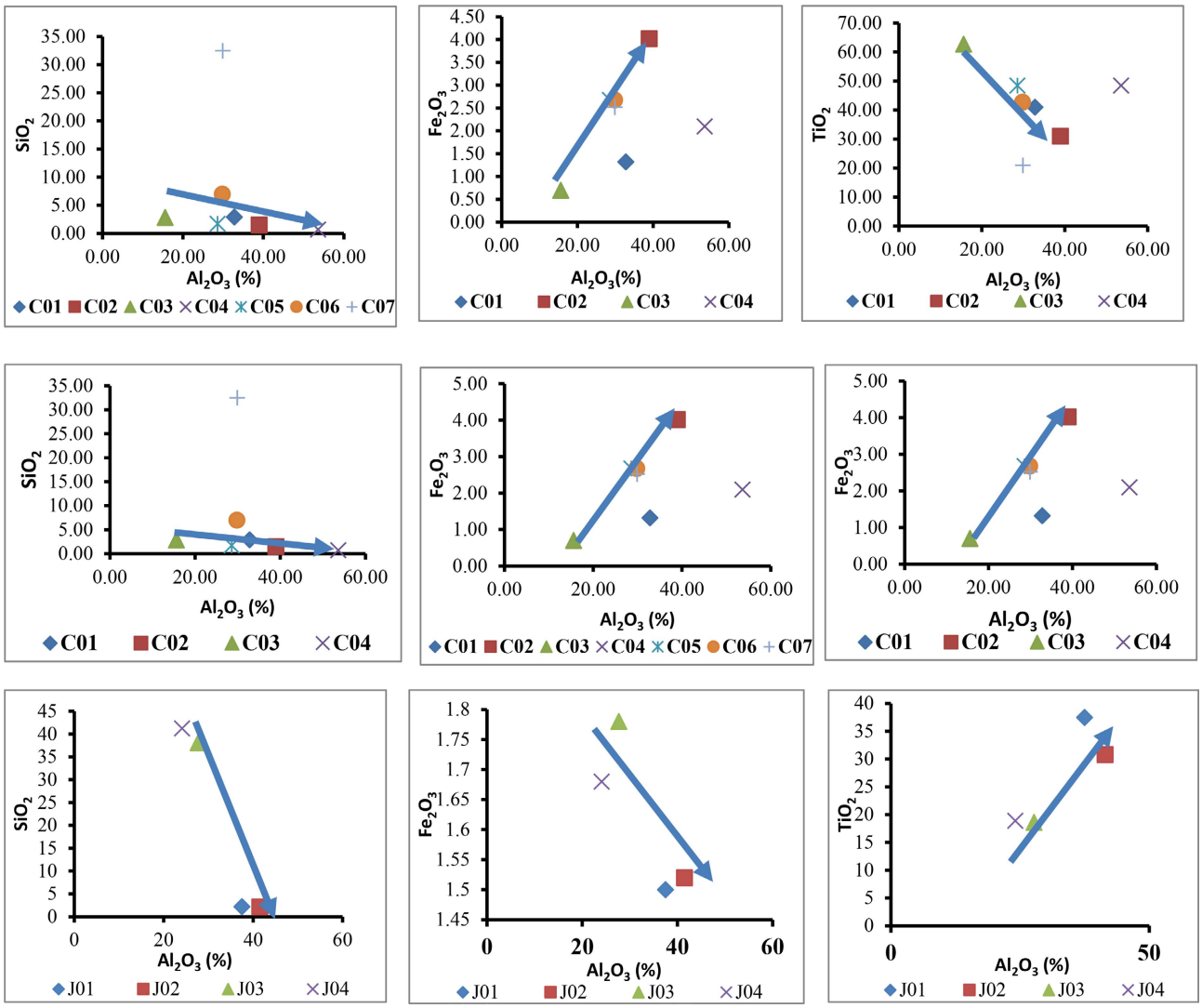

Figure 11. Correlation diagrams of SiO_2-Fe_2O_3 and TiO_2 versus Al_2O_3.

5. Discussion

Aluminum consists mainly of the minerals gibbsite, boehmite and diaspore. Gibbsite $Al(OH)_3$ is the most abundant and easily observed mineral in bauxite (Lapparent, 1930). Laterites have preserved the textures, structures and volumes of the original source rocks (Nahon, 2003). All these minerals are economically profitable. Gibbsitic bauxites (Sidibe and Yalcin, 2019) are mainly found in tropical regions characterized by a hot and humid climate (Njoya et al., 2017). Diaspore has been found as a minor component in several types of bauxite in which it is accompanied by gibbsite and boehmite (dos Santos et al., 2016). The alumogoethite found in many bauxite deposits is a product of the substitution of Al^{3+}

by Fe^{3+} in the goethite and in the soil (Liu et al., 2012).

Geochemical deposition trajectories for (Beauvais, 1991) and (Tardy, 1997) of lateritic bauxites from the Boundou-Waadé bauxites suggest that bauxite is the product of kaolinite destruction. Therefore, the indirect bauxitization or decilicification of kaolinite (Boulange et al., 1990) in a hot, humid tropical climate (Nahon, 2003) is the main alteration mechanism for the gibbsite formation of bauxites from the Boundou-Waadé plateau. The degree of laterization of (Schellmann, 1986) shows the degree of bauxitization. Bauxitic samples are highly lateritized (Sidibe and Yalcin, 2019; Zamanian et al., 2016); while the clayey ones are weakly lateritized (Zarasvandi et al., 2012) see kaolinized (this work).

In the diagram (Aleva, 1994) bauxitic samples are generally in the bauxite, kaolinitic bauxite and ferric bauxite fields (Zamanian et al., 2016); ferric samples in the bauxitic ferrite, ferrite and kaolinitic ferrite fields (Sidibe and Yalcin, 2019); clay samples in the kaolinite, bauxitic kaolinite and ferric kaolinite fields (Zamanian et al., 2016); laterite clay bauxites in the laterite field.

Correlation analysis showed a positive correlation between Al_2O_3 and TiO_2, Fe_2O_3 and Al_2O_3 and a negative correlation between SiO_2 and Al_2O_3; in bauxite. This is explained by the leaching of Si, the migration and accumulation of iron to form ferrites and residual enrichment of aluminium and titanium during the weathering process (**Figure 11**) (Zamanian et al., 2016). The high titanium oxide values are probably linked to the abundance of minor Ti minerals (rutile, anatase) in bauxites. While high iron values in bauxite samples are linked to the presence of iron-bearing minerals such as hematite, goethite and alumogoethite, formed under suitable Eh-PH conditions during the weathering process (Gu et al., 2013).

6. Conclusion

The aim of this study, which focuses on the petrographic, mineralogical, geochemical and statistical characterization of the Boundou-Waadée bauxite deposit, was to investigate the different types of bauxite and their source rocks.

Petrographically, the Boundou-Waadée deposit is essentially composed of lateritic bauxites derived from Devonian aleuro-argillite, argillite and aleurolite, as well as Mesozoic dolerites; and chemogenic bauxites resulting from the chemical redistribution of elements at the base of lateritic bauxites.

Mineralogically, we note the presence of gibbsite, goethite and alumogoethite. Diaspore and boehmite are absent from the bauxite horizon; kaolinite, quartz and hydromica are found in the clay horizon. Minor minerals include anatase, rutile and chlorite.

From a geochemical point of view, the different types of triangular diagrams of the major elements show that the BW bauxite deposit follows the destructive trend of kaolinite during the bauxitization process, and that bauxites, ferruginous laterites and ferriplantites are strongly lateritized, whereas clays and aleuro-argilites are weakly lateritized.

These materials are characterized by high Al_2O_3 contents, the Fe_2O_3 content is

highest in the ferrite samples (73.5%) and in sample J04 the SiO_2 content is quite high (41.25%). Whereas, the amount of TiO_2 varies, hence the presence of anatase. The gibbsite is the majority mineral (68.4%) in the materials studied. Accessory minerals include kaolinite, anatase and diaspore. Based on their chemical and mineralogical composition, these materials can be used for aluminum production. Statistical analysis was used to determine trends in bauxite composition in the study area. With the application of these methods, we can conclude that local changes in chemical composition and its variability could be determined more precisely. However, for the valorization of large quantities of minerals (titanium, kaolinite, clay...) in eco-construction and ceramics will be the subject of future studies with a view to finding a lasting solution to the housing and employment crisis currently raging in Boké. The study concludes that CBG's future production will be residual bauxite, 75% of the bauxite reserves in the Boundou-Waadé deposit. This residual type is derived from the alteration of Mesozoic argillites, aleuro-argillites and dolerites.

Acknowledgements

At the end of our work on the petrographic, mineralogical, geochemical and statistical characterization of the Boundou-Waadé bauxite deposit, we would like to thank the Ministry of Higher Education, Scientific Research and Innovation for their support. We would also like to thank the General Management of the Institut Supérieur des Mines et Géologie de Boké for their invaluable support, and the Compagnie des Bauxites de Guinea for their frank collaboration.

I would like to thank my thesis supervisor for his support, confidence and encouragement, and for his unstinting guidance throughout this study.

I would like to express my sincere gratitude and appreciation to Mme. Finda Kabama TEMESSADOUNO, Dre Marie Constance BEAVOGUI, Dr Mamoudou DIALLO, Mr. Yaya Kenda Baillo DIALLO, Mr. Pétoyi Paul MAOMY and Youssouf CAMARA for their support and advice in bringing this article to fruition.

Conflicts of Interest

This article presents no conflict of interest, and the authors wish to have the work published in this journal.

References

Aleva, G. J. J. (1994). Laterites: Concepts, Geology, Morphology and Chemistry. In International Soil Reference and Information Center (ISRIC) (Ed.), *The Corlat Handbook* (pp. 8-21). Corlat Technical Publication.

Beauvais, A. (1991). *Paleoclimates and Dynamics of a Battleship Landscape of the Central African Republic: Morphology, Petrology and Geochemistry.* Ph.D. Thesis, University of Poitiers.

Bhukte, P. G., Daware, G. T., Masurkar, S. P., Mahendiran, P., Janbandhu, K., Rao, K. R., Singh, U., Puttewar, S. P., & Agnihotri, A. (2020). Geochemical, Mineralogical and

Petrological Characteristics of Lateritic Bauxite Deposits Formed on Deccan Trap Basalt with Reference to High-Level and Coastal (Low Level) Deposits of Maharashtra. *Journal of the Geological Society of India,* 95, 587-598. https://doi.org/10.1007/s12594-020-1485-1

Boufeev, Y., Kriatov, B., & Kazakevitch, A. (1970). *Carte géologique de République de Guinée à l'échelle 1/200.000. Feuille Boffa et Notice Explicative* (p. 145). Rapport Organisme Soviétique de Recherche Géologique.

Boulange, B., Bouzat, G., & Pouliquen, M. (1996). Mineralogical and Geochemical Characteristics of Two Bauxitic Profiles, Fria, Guinea Republic. *Mineralium Deposita, 31,* 432-438. https://doi.org/10.1007/s001260050050

Boulange, B., Carvalho, A., & Melfi, A. (1990). *Geochemistry of the Earth's Surface and of Mineral Formation*, 32 p.

Bruno Boulanger, B., & Millot, G. M. (1988). La distribution des bauxites sur le Craton ouest-Africain. *Sciences Géologiques, bulletins et mémoires, 41,* 113-123. https://doi.org/10.3406/sgeol.1988.1785

dos Santos, P. H. C., Costa, M. L., & da Leite, A. S. (2016). Federal University of Para, Brazil, UFPA, Brazil, Vale Institute of Technology, Brazil, 2016. The Piria Aluminous Lateritic Profile: Mineralogy, Geochemistry and Parent Rock. *Brazilian Journal of Geology, 46,* 617-636. https://doi.org/10.1590/2317-4889201620160101

Gu, R., Duan, F., An, X., Zhang, F., von Wiren, N., & Yuan, L. (2013). Characterization of AMT-Mediated High-Affinity Ammonium Uptake in Roots of Maize (*Zea mays* L.). *Plant and Cell Physiology, 54,* 1515-1524.

Lapparent, J. (1930). The Minerals of French Bauxites. *Company Fr. Mineralogy, Bulletin de Mineralogie, 53,* 255-273. https://doi.org/10.3406/bulmi.1930.4096

Liu, X., Wang, Q. F., Zhang, Q. Z., Feng, Y. W., & Cai, S. H. (2012). Mineralogical Characteristics of the Superlarge Quaternary Bauxite Deposits in Jingxi and Debao Counties, Western Guangxi, China. *Journal of Asian Earth Sciences, 52,* 53-62. https://doi.org/10.1016/j.jseaes.2012.02.011

Mamedov, V. I., Boufeev, Y. V., Nikitine, Y. A., & Mamedov, A. I. (2010). *Bank of Useful Mineral Deposits and Index Data.* Geoprospects LTD; Univ. Moscow State Council, Aquarel, Moscow, 264 p.

Nahon, D. (2003). Altérations dans la zone tropicale. Signification à travers les mécanismes anciens et/ou encore actuels. *Comptes Rendus Geoscience, 335,* 1109-1119. https://doi.org/10.1016/j.crte.2003.10.008

Njoya, D., Njoya, A., Ngueteu, A. K., Tchuindjang, Y. D., & Nkoumbou, C. (2017). Caractérisation chimique et minéralogique de quelques indices de bauxite de Foumban (Ouest-Cameroun). *International Journal of Biological and Chemical Sciences, 11,* 444-452. https://doi.org/10.4314/ijbcs.v11i1.35

Samozvantsev, V., Diallo, H., & Balachov, B. (1976). *Carte géologique de République de Guinée à l'échelle 1/200.000. Feuille Kandiafara et Notice Explicative* (p. 156). Rapport Société d'Exploration Géologique Fédération de Russie-Organisme de Recherche Géologique.

Schellmann, W. (1986). On the Geochemistry of Laterites. *Chemie der Erde, 45,* 39-52.

Seliverstov, Y. P. (1970). *Carte géologique de Republique de Guinée à l' échelle 1/200.000. Feuille Télémélé Notice Explication* (p. 135). Rapport Organisme Soviétique de Recherche Géologique.

Sidibe, M., & Yalcin, M. G. (2019). Petrography, Mineralogy, Geochemistry and Genesis of the Balaya Bauxite Deposits in Kindia Region, Maritime Guinea, West Africa. *Journal of*

African Earth Sciences, 149, 348-366. https://doi.org/10.1016/j.jafrearsci.2018.08.017

Tardy, Y. (1997). *Petrology of Laterites and Tropical Soils* (408 p). AA Balkema.

Zamanian, H., Ahmadnejad, F., & Zarasvandi, A. (2016). Mineralogical and Geochemical Investigations of the Mombi Bauxite Deposit, Zagros Mountains, Iran. *Geochemistry, 76,* 13-37. https://doi.org/10.1016/j.chemer.2015.10.001

Zarasvandi, A., Carranza, E. J. M., & Ellahi, S. S. (2012). Geological, Geochemical, and Mineralogical Characteristics of the Mandan and Deh-Now Bauxite Deposits, Zagros Fold Belt, Iran. *Ore Geology Reviews, 48,* 125-138. https://doi.org/10.1016/j.oregeorev.2012.02.010